Article

pubs.acs.org/Biomac

# Formation of Cucurbit[8]uril-Based Supramolecular Hydrogel Beads Using Droplet-Based Microfluidics

Xuejiao Xu,[†] Eric A. Appel,[‡] Xin Liu,[†] Richard M. Parker,[†] Oren A. Scherman,*[,‡] and Chris Abell*[,†]

[†]Department of Chemistry and [‡]Melville Laboratory for Polymer Synthesis, Department of Chemistry, University of Cambridge, Lensfield Road, Cambridge CB2 1EW, United Kingdom

Supporting Information

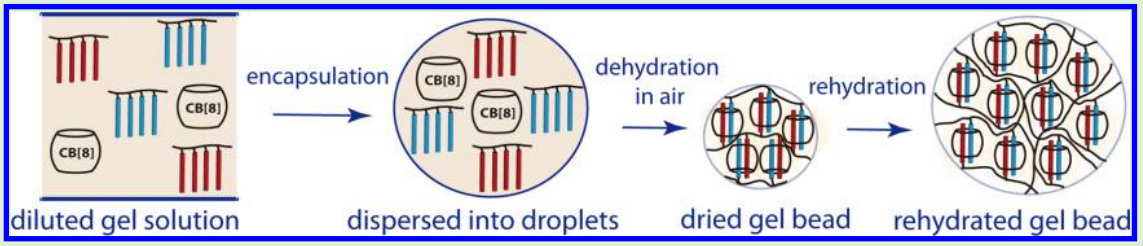


**ABSTRACT:** Herein we describe the use of microdroplets as templates for the fabrication of uniform-sized supramolecular hydrogel beads, assembled by supramolecular cross-linking of functional biopolymers with the macrocyclic host molecule, cucurbit[8]uril (CB[8]). The microdroplets were formed containing diluted hydrogel precursors in solution, including the functional polymers and CB[8], in a microfluidic device. Subsequent evaporation of water from collected microdroplets concentrated the contents, driving the formation of the CB[8]-mediated host−guest ternary complex interactions and leading to the assembly of condensed three-dimensional polymeric scaffolds. Rehydration of the dried particles gave monodisperse hydrogel beads. Their equilibrium size was shown to be dependent on both the quantity of material loaded and the dimensions of the microfluidic flow focus. Fluorescein-labeled dextran was used to evaluate the efficacy of the hydrogel beads as a vector for controlled cargo release. Both passive, sustained release (hours) and triggered, fast release (minutes) of the FITC-dextran was observed, with the rate of sustained release dependent on the formulation. The kinetics of release was fitted to the Ritger-Peppas controlled release equation and shown to follow an anomalous (non-Fickian) transport mechanism.

## INTRODUCTION

Hydrogels consist of three-dimensional networks of hydrophilic polymer chains. This porous structure can accommodate a high volume of water that not only gives the gel form, but allows for the storage of hydrophilic biomolecules.[1] Hydrogels have been shown to have highly tunable mechanical properties and good biocompatibility, making them increasingly important in a variety of biomedical applications, including tissue engineering,[2,3] wound management, drug delivery,[3,4] and diagnostic devices.[5] In drug delivery, there are potential in vivo applications for materials supplying a sustained and controlled dose of therapeutic cargo at a specific site, as well as those allowing for triggered, rapid delivery of cargo.[6]

Droplet-based microfluidics provide a route to a versatile and powerful fabrication approach that provides a platform for the generation of emulsified microdroplets with extremely low polydispersity.[7] This approach has been implemented in the fabrication of hydrogel beads, whereby monodispersed microdroplets are used as a template for particle synthesis, with the size of the hydrogel particle controlled by tuning the size of microdroplets.[6,8,9] In contrast, conventional bulk emulsion-based methods produce microparticles with high polydispersity in both volume and encapsulation efficiency, with variation from batch to batch resulting in high variability of encapsulated drug release kinetics.[8,10] The microfluidic approach additionally offers the opportunity to uniformly load other substances inside the hydrogel particles.[11,12]

Several different materials have been reported in the synthesis of monodispersed hydrogel beads via droplet-based microfluidics. Synthetic polymers are typically used, with cross-links introduced through the addition of a chemical chelator[9] or by photoinitiated polymerization by ultraviolet (UV) illumination.[7,13−15] Natural biomaterials such as polysaccharides[16−19] and proteins[20−23] offer high biocompatibility, but suffer from several disadvantages, including inconsistencies in composition and difficult synthetic modifications for tailoring materials for specific applications. Recently, multicomponent systems have also been developed.[24]

Hydrogels prepared using highly specific, directional, and strong supramolecular interactions have been reported recently with gel formation shown to be both reversible and tunable by external stimuli.[1,25,26] The cucurbit[*n*]uril family of macrocycles (CB[*n*]) (*n* = 5−8, 10) can act as a cross-linking agent, accommodating scaffold-tethered guest moieties within its macrocyclic cavity. The size of the cuburbit[*n*]uril cavity is determined by the number of glycoluril units. While CB[5−7] are capable of accommodating a single guest,[27−29] CB[8] has a larger cavity volume of

Received: May 17, 2015
Published: August 10, 2015





DOI: 10.1021/acs.biomac.5b01048
*Biomacromolecules* 2015, 16, 2743−2749

479 Å$^3$ enabling it to accommodate one electron-deficient guest and one electron-rich guest simultaneously.[30−32] The resulting 1:1:1 heteroternary complex can be considered as a molecular "handcuff", linking two complementarily functionalized scaffolds together.[33] In comparison with conventional chemical and physical cross-linking methods for the preparation of hydrogel particles, this CB[8]-based ternary system is of particular interest in aqueous-based self-assembly on account of its dynamic nature combined with its high binding constants in water ($K_a \geq 10^{14}$ $M^{-2}$).[1,26,34] These hydrogels can be easily prepared from inexpensive renewable resources and exhibit high water content and biocompatibility. Moreover, external stimuli can trigger the reversible noncovalent interaction between host and guest, making it an ideal candidate for cargo delivery applications. This system has been used for the fabrication of microcapsules for various applications.[35,36] However, the fabrication of monodispersed supramolecular hydrogel particles of this kind and their use as a cargo delivery vector has not previously been investigated.

Here we demonstrate a simple method to fabricate monodisperse supramolecular hydrogel beads by taking advantage of the noncovalent interaction between CB[8] with methyl viologen- and 2-naphthyl-modified polymers, within a droplet-based microfluidic platform. The size of the formed hydrogel beads is shown to be tunable by varying either the initial polymer loading or the dimensions of the microfluidic flow focus junction. These particles demonstrate controlled and sustained release of cargo dependent on the relative loading of the polymers and CB[8] in the hydrogel formulation. Moreover, triggered rapid release of cargo is shown to be initiated through the disruption of the supramolecular cross-links, demonstrated by the addition of the strongly competing guest, 1-adamantylamine (ADA). These high water-content supramolecular hydrogel beads have potential applicability in cargo delivery by functioning as a site-specific delivery vector for both controlled, sustained release and triggered, rapid release of cargo.

## MATERIALS AND METHODS

**Materials.** Hydroxyethylcellulose (HEC) was purchased from Aldrich and dried overnight in a vacuum oven at 105 °C. ACPA was purchased from Sigma-Aldrich and was recrystallized from methanol. STMV[1] and cucurbit[8]uril[2] were prepared according to literature procedures. All other materials were purchased from Sigma-Aldrich and used as received.

**Synthesis of $HEC_{Np}$.** HEC (1.00g) was dissolved in *N*-methylpyrrolidone (NMP, 150 mL) at 110 °C. The solution was cooled to room temperature and Np-NCO (29.7 mg, 0.18 mmol) and dibutyltin dilaurate (3 drops) were added, and the mixture was allowed to stir at room temperature overnight. The functional polymer was then purified by precipitation from acetone, filtered, and dried overnight under vacuum at 60 °C (1.01 g, 98%). $^1$H NMR spectroscopy ($D_2O$, 500 MHz) $\delta$ (ppm) = 7.99−7.29 (7H, br, Np-*H*), 4.60−2.75 (4.55H, br, cellulose backbone). Elem. ($C_{85.5}H_{144.2}O_{60.6}N_1$): Found C, 47.14; H, 6.93; N, 0.68; Calcd. C, 47.63; H, 6.74; N, 0.65. FT-IR (ATR) $\upsilon$ = 3410 (br), 2950 (br), 2910 (br), 1395, 1075 (s) cm$^{-1}$. GPC ($H_2O$): $M_n$ (PDI) = 3.4 MDa (1.25).

**Synthesis of $SAM_{MV}$.** 1-Methyl-1′-(4-vinylbenzyl)-[4,4′-bipyridine]-1,1′-diium chloride iodide (STMV; 0.35 g, 0.78 mmol), (vinylbenzyl)trimethylammonium chloride (SAM; 1.47 g, 6.99 mmol), and 4,4′-azobis(4-cyanopentanoic acid) (ACPA; 10.9 mg, 38.9 $\mu$mol) were dissolved in a 1:1 ($v/v$) mixture of deionized water and ethanol (5.2 mL) in a Schlenk tube, and the solution was degassed by bubbling nitrogen for 30 min. The Schlenk tube was then sealed and heated in an oil bath set to 70 °C for 48 h. The reaction was quenched in liquid nitrogen, and the polymer was isolated by precipitation from cold diethyl ether, filtered, and dried under vacuum to afford the title compound as a yellow amorphous solid (1.75 g, 96%). $^1$H NMR spectroscopy ($D_2O$, 500 MHz) $\delta$ (ppm) = 9.18−8.88 (4H, br, MV aryl-*H*), 8.60−8.33 (4H, br, MV aryl-*H*), 7.73−6.11 (18.8H, br, St-*H*), 5.96−5.58 (2H, br, MV-C$H_2$), 4.64−3.98 (18.7H, br, MV-C$H_3$ and St-C$H_2$-AM), 3.24−0.3 (107.3H, br, polymer backbone). GPC ($H_2O$): $M_n$ (PDI) = 37.1 kDa (2.42).

**Device Fabrication.** Devices were fabricated using soft lithography.[3] The devices were first designed using AutoCAD and printed to high-resolution photomasks. Photoresist SU-8 2025 (MicroChem) was spin-coated onto a 3″ silicon wafer, followed by incubation. The resulting wafer was then placed on a mask aligner (Süss MicroTec), covered with photomask, and exposed to UV light (365 nm) to engrave the pattern of the mask on the wafer before further baking. Once complete, the wafer was submerged in the propylene glycol monomethyl ether acetate (PGMEA) developer and rinsed by 2-propanol, followed by baking (1 min), to stabilize the pattern.

Mixed prepolymer Sylgard 184 (Dow Corning) and its curing agent in a ratio 10:1 (w/w) was poured onto the wafer and degassed in a desiccator for 1 h. The unit was placed in an oven at 80 °C for 6 h. Once cured, the PDMS was peeled from the wafer and punched with a biopsy punch (Kai Industries) with an outer diameter of 1 mm. The PDMS was then bonded to a glass slide with plasma treatment in a Femto plasma cleaner (Diener electronic) for 8 s. The fluorophilic behavior of the internal channel was achieved by flushing with Aquapel (Duxback). Finally, the device was placed in a 100 °C oven for 4 h and cooled to room temperature for use.

**Preparation of Hydrogel Beads without Model Cargo.** Microdroplets were generated in a flow-focusing device with a single aqueous inlet. The nozzle size was 75 $\mu$m in depth and 60 $\mu$m in width with oil and the aqueous phase flow rate of 500 and 50 $\mu$L/h, respectively. The aqueous phases consisted of a diluted mixture of polymer $HEC_{Np}$, $SAM_{MV}$, and CB[8]. The oil phase comprised the surfactant Pico-Surf$^{TM}$ 1 dissolved in the perfluorinated oil, HFE 7500. The generated droplets were collected on a glass microscope slide for analysis and allowed to evaporate in air. Subsequent rehydration in water was achieved by adding 30 $\mu$L of deionized water to the surface, allowing the dehydrated particles to form the desired hydrogel beads. The generation of microdroplets, the formation of dehydrated hydrogel beads and the process of rehydration was analyzed under bright-field via a monochrome Phantom v7.2 camera (Vision Research) mounted to an IX 71 inverted microscope (Olympus).

**Preparation of Hydrogel Beads with Model Cargo.** In the cases where cargo was loaded, 0.1 mg/mL of FITC-dextran of the desired molecular weight was premixed in the diluted aqueous gel solution. After the dehydration and rehydration process, the fluorescence variation in hydrogel beads was imaged using an EM-CCD camera (iXionEM+, Andor Technologies), which was connected to an inverted microscope IX 71 (Olympus) operating in both bright-field and epifluorescence mode. Custom Labview software was used to trigger an EM-CCD camera to visualize both bright-field and fluorescence images every 15 min. In the visualization of both bright-field and fluorescence images, light from a wide-field illuminating mercury lamp (U-LH100HG, Olympus) was passed through FITC filters and dichroics to separate the light used for excitation from the fluorescence emission of FITC-dextran.

**Triggered Release by a Competitive Guest.** Hydrogel beads loaded with 10kDa FITC-dextran were fabricated as described in the previously section. After rehydration in deionized water, a few drops (~10 $\mu$L) of 2 mM 1-adamantaneamine (ADA) solution was introduced and the fluorescence micrograph recorded every 15 min (automated via custom Labview software) to track release of the FITC-tagged cargo.

For flow control in all the microfluidic experiments, 1 mL SGE glass syringes were driven by syringe infusion pumps (Harvard Apparatus 2000) and connected to the device by polyethylene tubing (inner diameter, 0.38 mm; Intramedic).

## RESULTS AND DISCUSSION

**Fabrication of Supramolecular Hydrogel Beads.** As illustrated in Figure 1A, supramolecular hydrogel formation is



DOI: 10.1021/acs.biomac.5b01048
*Biomacromolecules* 2015, 16, 2743−2749

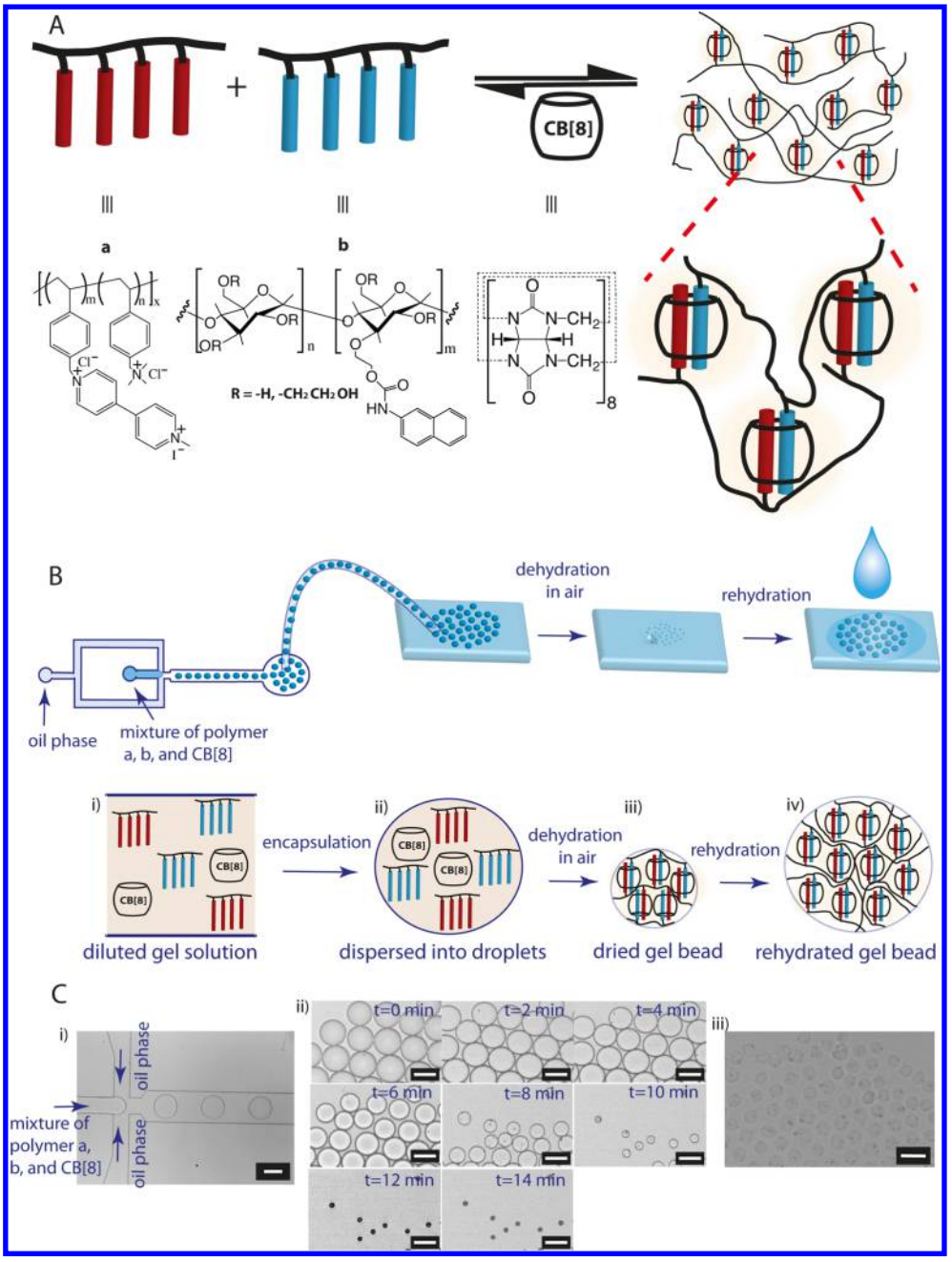


**Figure 1.** (A) Schematic representation of the formation of a supramolecular cross-linked hydrogel through the addition of CB[8] to a mixture of methyl viologen (red) functionalized poly((vinylbenzyl)trimethylammonium chloride) copolymer ($SAM_{MV}$) and naphthyl (blue) functionalized poly(hydroxyethyl cellulose) copolymer ($HEC_{Np}$). (B) A schematic illustration of the process of hydrogel bead generation; (i) microdroplets containing a dilute mixture of polymers ($SAM_{MV}$ and $HEC_{Np}$) and CB[8] were generated in a flow-focusing device with an oil/water flow rates of 500 and 50 $\mu L \cdot h^{-1}$, respectively, (ii) the droplets were collected on a microscope slide and (iii) allowed to evaporate to form a dehydrated hydrogel particle over 14 min at room temperature (iv) upon rehydration with water (~30 $\mu$L), monodisperse hydrogel beads were obtained. (C) Corresponding bright-field micrographs of the hydrogel particle fabrication process: (i) microdroplet generation, (ii) evaporation to form a hydrogel particle, and (iii) rehydration to form swollen hydrogel beads. The droplets were generated with $SAM_{MV}$ concentration of 0.38 mg/mL, $HEC_{Np}$ of 1.25 mg/mL and CB[8] of 0.25 mg/mL in a device with flow-focusing junction dimension of 75 $\mu$m in depth, 60 $\mu$m in width. Scale bar indicates 50 $\mu$m.

driven through the cross-linking of the polymer network via a ternary host−guest interaction between CB[8] and both polymer-bound methyl viologen and naphthol moieties. The methyl viologen (MV) functionalized polymer ($SAM_{MV}$) was synthesized via copolymerization of a methyl viologen-modified styrenic monomer and water-soluble (vinylbenzyl)trimethylammonium chloride comonomer by traditional free radical polymerization.[1] Naphthyl (Np) functionalized polymer ($HEC_{Np}$) was synthesized by conjugation of an isocyanate-functional Np moiety to poly(hydroxyethyl cellulose), which had a number-average molecular weight of 1.3 MDa.[26] The successful formation of bulk hydrogel from the 1:1:1 mixture of these polymers based on guest concentration with CB[8] is demonstrated in Figure S1.

To form hydrogel beads from these polymeric precursors, a stepwise procedure was followed (Figure 1B): (i) generation of aqueous microdroplets containing a dilute mixed solution of functional copolymers and CB[8] via a microfluidic flow focus junction, (ii) subsequent collection of generated droplets, (iii)


DOI: 10.1021/acs.biomac.5b01048
Biomacromolecules 2015, 16, 2743−2749

evaporation of the aqueous phase leading to an increase in concentration promoting supramolecular cross-linking within the droplet, and (iv) rehydration in deionized water to produce monodisperse hydrogel beads.

The microfluidic device, comprising of a flow-focusing junction and a single aqueous and oil inlet, was fabricated from poly(dimethylsiloxane) and treated to give a fluorophilic channel surface. The carrier phase comprised of HFE 7500 fluorocarbon oil with 2% Pico-Surf 1 surfactant. The aqueous solution contained a mixture of 0.38 mg/mL $SAM_{MV}$, 1.25 mg/mL $HEC_{Np}$, and 0.25 mg/mL CB[8], and was warmed (~40 °C) to lower the viscosity on a temperature-controlled microscope heating stage. With an oil/water flow rate ratio of 10:1 (500 and 50 $\mu L \cdot h^{-1}$, respectively), aqueous microdroplets with a diameter of 65 $\mu$m were generated within the oil carrier flow at the flow-focusing junction (Figure 1C-i). The generated droplets were then collected on a glass microscope slide for analysis. The aqueous phase was allowed to evaporate in air over 14 min at room temperature, leading to a dramatic reduction in droplet size to a diameter of ~15 $\mu$m (Figure 1C-ii). During this process, concentration of the functional polymers with the CB[8] host promoted cross-linking to form compact, spherical hydrogel particles. Rehydration of these hydrogel particles led to the formation of uniformly sized, high water content hydrogel beads (Figure 1C-iii), with a doubling in diameter from the dehydrated state to rehydrated state observed after 1 min.

The effect of altering the initial material loading within the droplet upon the size and swelling behavior of the resultant hydrogel beads was investigated by altering either the microfluidic channel geometry or the component composition. It was found that maintaining the composition of the aqueous flow resulted in larger hydrogel beads being formed when the size of the templating microdroplet was increased. As shown in Figure S2, larger hydrogel beads were formed when increasing device aperture dimension. A similar trend was observed when the material loadings of polymer $SAM_{MV}$, $HEC_{Np}$, and CB[8] were increased while maintaining a constant, equimolar ratio of $SAM_{MV}/HEC_{Np}$/CB[8] components. Transmission optical micrographs of the hydrogel beads under these conditions are given in Figures S2−4.

The efficiency of the CB[8] cross-link in maintaining the hydrogel bead structure upon rehydration was investigated by varying the relative CB[8] concentration within the microdroplet from 0 to 1 equiv. relative to the concentration of polymer-bound guest. It was found that, while the diameter of the hydrogel particles formed upon evaporation of the microdroplet was similar irrespective of CB[8] concentration, the swelling behavior upon rehydration differed markedly, as shown in Figure 2. In the absence of CB[8], the particles swelled about 25% during the first minute after rehydration, but were later observed to break, with the polymers gradually dispersing into the aqueous media over time. In contrast, 0.5 equiv. of CB[8] loading resulted in the formation of stable hydrogel particles over the same period, while further increasing CB[8] to 1.0 equiv. led to the production of stable hydrogel particles with a greater degree of swelling. This is attributed to the CB[8]-mediated host−guest supramolecular cross-linking of the polymer beads, where in the absence of CB[8] the polymers will slowly dissolve. Substoichiometric concentrations of CB[8] only partially cross-link the polymers loaded within the microdroplet during the dehydration process, allowing unbound polymer to diffuse away during rehydration, leading to formation of smaller beads. In comparison, hydrogel beads formed with 1.0 equiv. of CB[8],

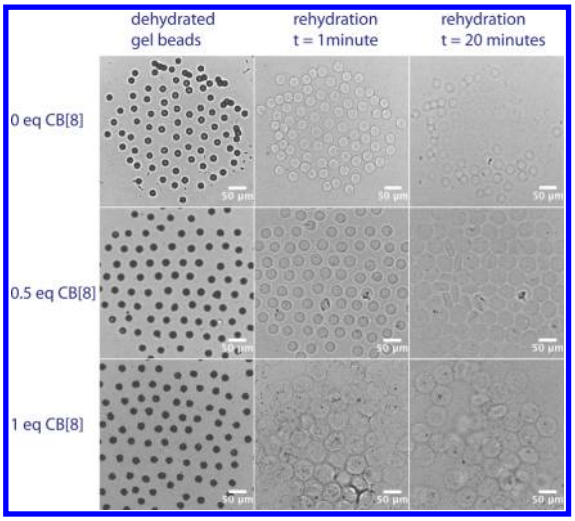


**Figure 2.** Bright-field images of dehydrated hydrogel particles and after rehydration for 1 and 20 min when loaded in the absence of CB[8], with 0.5 equiv CB[8], and 1 equiv CB[8]. Scale bar indicates 50 $\mu$m. The droplets were generated with $SAM_{MV}$ concentration of 0.375 mg/mL, $HEC_{Np}$ of 1.25 mg/mL, and CB[8] of 0, 0.125, and 0.25 mg/mL, respectively.

where most of the polymers in an individual droplet are "handcuffed" via supramolecular noncovalent cross-linking between complementary polymer chains, are robust and readily swell to stable particles upon rehydration.

**Controlled, Sustained Delivery of a Model Cargo.** The viability of the supramolecular hydrogel beads as a cargo delivery vector for macromolecular cargoes was investigated. Fluorescein-tagged dextran (FITC-dextran), used as a model cargo, was loaded into the microgel beads during droplet formation, with the release kinetics during rehydration monitored by fluorescence microscopy. Hydrogel beads were first fabricated with 1 equiv. of CB[8] containing FITC-dextran (0.1 mg/mL and 10 kDa). As shown by the time-lapse fluorescent microscopic images, Figure 3, row 4 (1 equiv. of CB[8]), a small proportion of the loaded cargo diffused quickly out of the hydrogel beads during the swelling process. This initial "burst" release was followed by a sustained release from hydrogels once rehydration and swelling were completed. To expand upon this, a series of hydrogel beads were prepared with CB[8] loading increasing from 0 to 2 equiv., with the remaining hydrogel components kept constant. Fluorescent micrographs recording the release of 10 kDa FITC-dextran from this series are presented in Figure 3. As before, in the absence of CB[8] the hydrogel beads dissipated completely after 30 min with the loaded cargo fully dispersed into the bulk aqueous media (Figure 3, row 1). An increase in hydrogel particle stability and a decreasing cargo release rate were observed with increasing cross-link density (see rows 2−5 of Figure 3), achieved by increasing the amount of CB[8]. It was observed that for 0.25 and 0.5 equiv. of CB[8] the release of cargo was completed within 3 and 4.5 h, respectively. The release of FITC-dextran was much slower when the hydrogel beads are prepared with 2 equiv. of CB[8], which resulted in more compact (i.e., less swollen) and more highly cross-linked hydrogel beads.

To further understand the process of cargo release from these hydrogel beads, the fluorescence intensity profiles of the beads illustrated in Figure 3 were quantified using ImageJ software.[37] The cumulative cargo release for hydrogel particles formulated with 0.25, 0.5, 1, and 2 equiv. of CB[8] were plotted over time


DOI: 10.1021/acs.biomac.5b01048
Biomacromolecules 2015, 16, 2743−2749

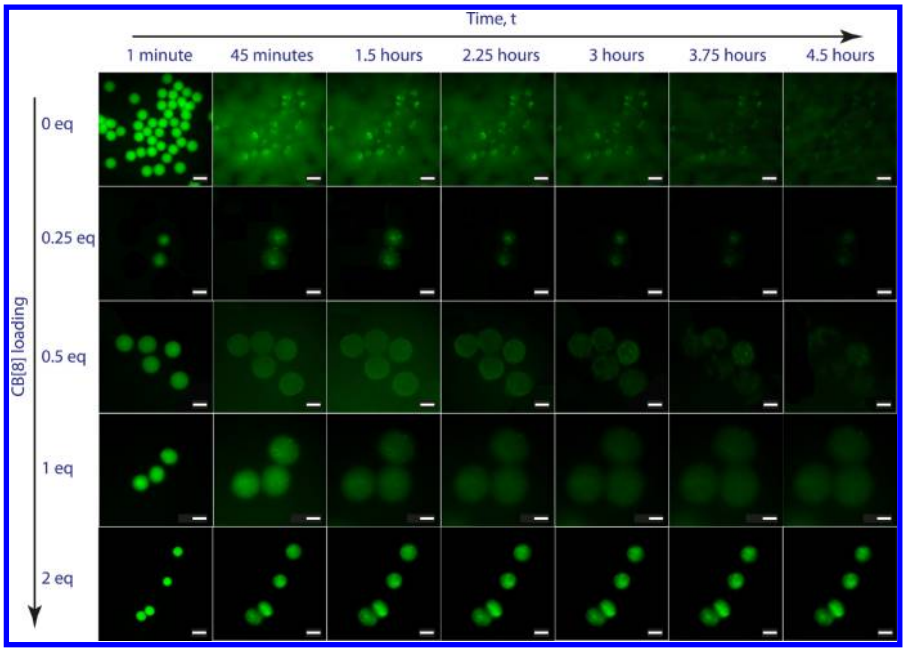


**Figure 3.** Fluorescence micrographs illustrating the release of the model cargo, FITC-dextran (10 kDa, loaded at 0.1 mg/mL in the original droplet formulation) over time from supramolecular hydrogel particles formed with differing amounts of CB[8]. Rows from top to bottom illustrate increasing loading of CB[8] in the droplet formulation, with a corresponding increase in retention of FITC-dextran cargo. Scale bars indicate 50 $\mu$m.

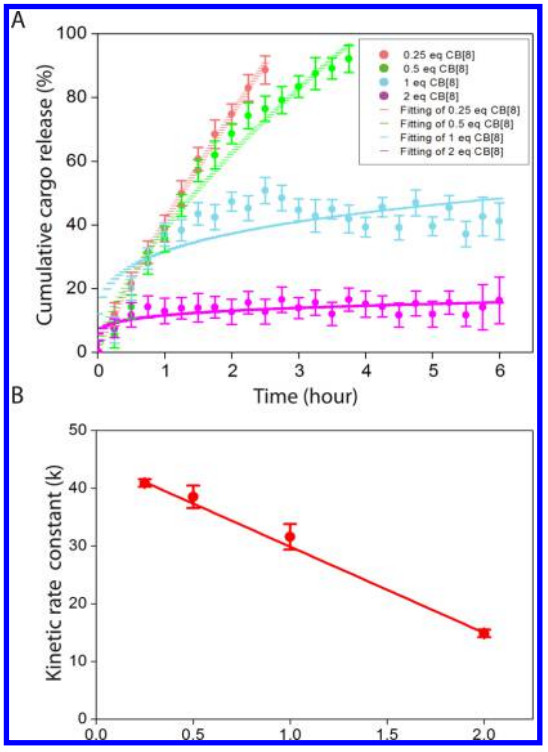


**Figure 4.** (A) Release kinetics of 10 kDa FITC-dextran from hydrogel beads fabricated with one equimolar of polymers (0.38 mg/mL $SAM_{MV}$, 1.25 mg/mL $HEC_{Np}$) and different loadings of CB[8] (0–0.25 mg/mL). Red, green, blue, and purple solid circles represent beads made with 0.25, 0.5, 1, and 2 equiv of CB[8], respectively. Fittings based on the Ritger-Peppas controlled release equation under the four conditions are indicated by dashed lines in the corresponding colors. (B) The relationship between the release rate derived from the fitted data and the CB[8] loading in the hydrogel bead formulation. Error bars indicate standard error averaged from 30 hydrogel beads.

(Figure 4A), with each series representing the mean release profile of over 30 hydrogel beads. Release behavior was fitted to the Ritger-Peppas controlled release eq (Figure 4A) for solute release from polymeric devices: $M_t/M_\infty = kt^n$, where $M_t/M_\infty$ is the fraction of cargo released, $k$ is the kinetic rate constant, and $n$ is the diffusional exponent of drug release.[38−40] The diffusional exponent $n$ raised from 0.50 to 0.87 when increasing the loading of CB[8] in hydrogel from 0.25 to 2 equiv. (Table S1). The value of $n$ is in the range from 0.43 to 0.89, indicating an anomalous (non-Fickian) release mechanism.[38−40] This is possibly due to the swelling and erosion of the hydrogel beads as well as the diffusion of loaded cargo. The release rate constants $k$ decreased from 40.9 to 14.9 when the loading of CB[8] in hydrogel increased from 0.25 to 2 equiv. (Table S1), plotting $k$ as a function of CB[8] loading, a linear correlation was observed (Figure 4B) in accordance with our previous observations from the fluorescence microscopy study (Figure 3). The lower release rate was due the more compact and higher cross-linking of hydrogel beads with increasing amount of CB[8] loading.

This study was expanded to investigate the effect of cargo molecular weight (and correspondingly, the hydrodynamic radius) on the release rate from hydrogel beads assembled with 1 equiv. of CB[8]. Fluorescence micrographs were collected at 15 min intervals during rehydration of hydrogel beads loaded with FITC-dextran with molecular weights: 4, 7, 10, 150, and 500 kDa (Figures 5A and S5). The fluorescence intensity of each time-resolved series was quantified and averaged as before, with the cumulative release of cargo plotted against time (Figure 5B). The release rate decreased with increasing molecular weight of FITC-dextran from 4 to 500 kDa. While 90% of the 4 kDa FITC-dextran was released from the hydrogel beads in 2 h, this increased to 3.5 h for the 7 kDa FITC-dextran. Dramatically decreased release rates were observed for hydrogel particles containing FITC-dextran larger than 10 kDa. After the initial release of cargo during the swelling (which again decreased with increasing cargo mass from 40% with 10 kDa to 15% with 500 kDa), negligible further release was observed over the course of the experiment.

**Triggered, Rapid Release of a Model Cargo.** The CB[8]-based supramolecular cross-linking is both dynamic and stimuli



DOI: 10.1021/acs.biomac.5b01048
*Biomacromolecules* 2015, 16, 2743−2749

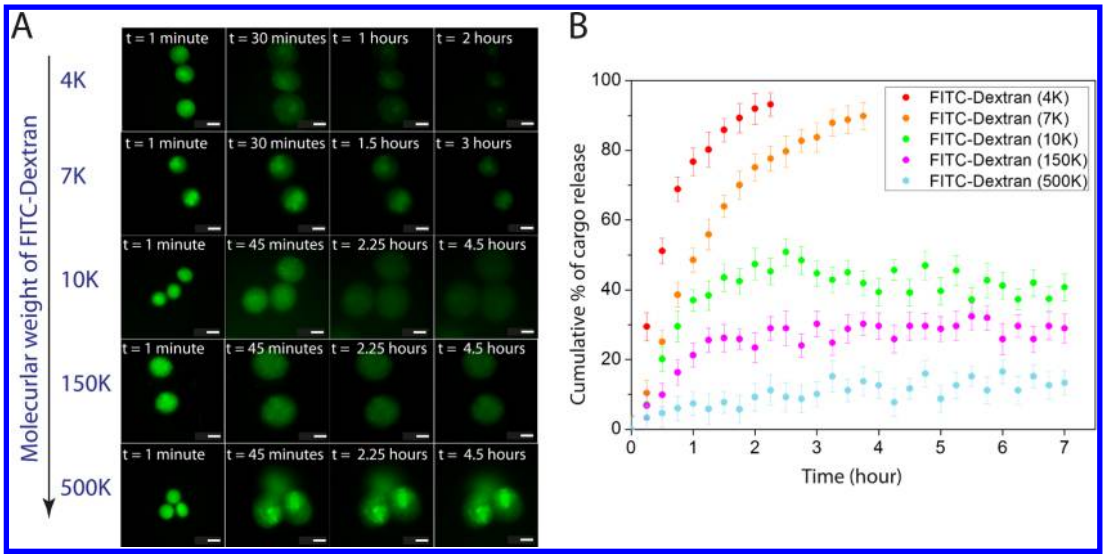


**Figure 5.** (A) Fluorescence micrographs illustrating the release of FITC-dextran cargo with molecular weight from 4 to 500 kDa (loaded at 0.1 mg/mL in the original formulation) over time from supramolecular hydrogel particles formed with one equimolar of polymers and CB[8] (0.38 mg/mL $SAM_{MV}$, 1.25 mg/mL $HEC_{Np}$, and 0.25 mg/mL CB[8]). (B) Release kinetics of different molecular weight of FITC-Dextran (4−500 kDa) over time from the supramolecular hydrogel beads illustrated in (A). Red, orange, green, purple, and blue solid circles represent cargo molecular weight of 4, 7, 10, 150, and 500 kDa, respectively. Error bar indicates standard error from the average of 30 hydrogel beads.

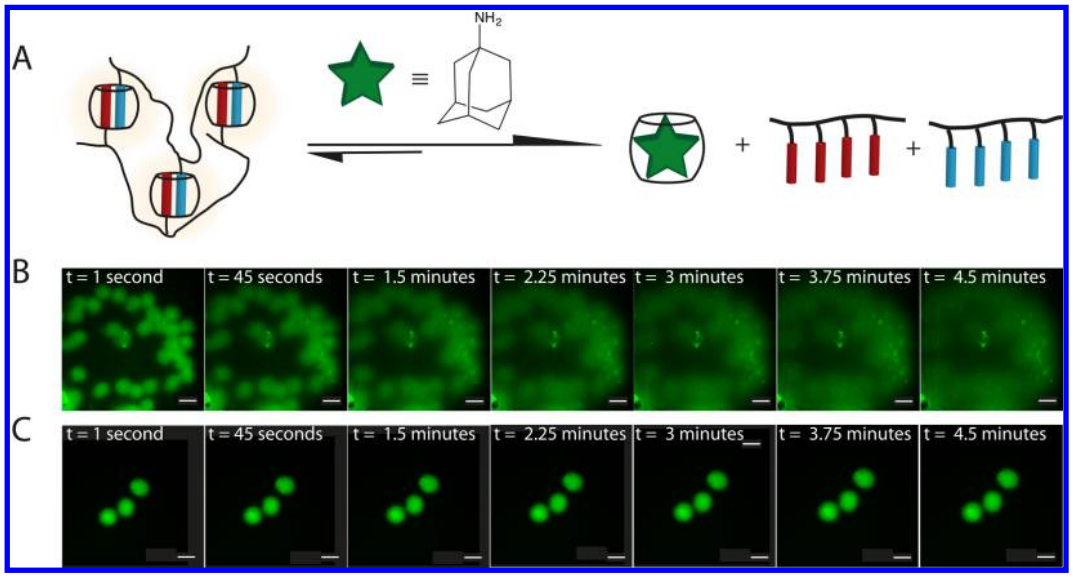


**Figure 6.** (A) Schematic illustration of triggered release from hydrogel beads with 10 $\mu$L of 1-adamantylamine (ADA) solution (2 mM). Time-resolved fluorescence micrographs comparing the release of FITC-dextran (10 kDa) from hydrogel beads made from one equimolar of polymers and CB[8] (0.38 mg/mL $SAM_{MV}$, 1.25 mg/mL $HEC_{Np}$, and 0.25 mg/mL CB[8]) by (B) triggered breakdown in ADA solution and (C) sustained swelling in water over 4.5 min. Scale bars indicate 50 $\mu$m.

responsive, making the release of cargo from hydrogel beads responsive external stimuli, such as a competitive guest that displaces the polymer-bound guest, as illustrated in Figure 6A.[26] The addition of 1-adamantylamine (ADA), which is a strongly competing guest ($K_{eq} = 1 \times 10^8$ $M^{-1}$) for the CB[8] host, was therefore studied as a trigger for controlled release of cargo.

The release of FITC-dextran (10 kDa) from hydrogel beads was investigated upon addition of aqueous ADA solution (2 mM; Figure 6B). Hydrogel beads started to dissipate immediately upon addition of a few drops (~10 $\mu$L) of ADA solution, with complete dissolution observed after 2 min. During this time, the FITC-dextran cargo was observed to rapidly diffuse into the aqueous media (Figure 6B). This behavior is in strong contrast to the hydrogel beads described earlier, which in the absence of ADA solution were observed to swell slightly with slow, sustained release of cargo over the same period (Figure 6C).

## CONCLUSION

In summary, monodisperse supramolecular hydrogel beads were synthesized based on CB[8]-mediated host−guest interactions within a droplet-based microfluidic platform. The formation of the selective ternary complex between CB[8] and two complementary guests leads to the formation of hydrogel beads with easily tunable features via modulation of the droplet formulation or microdroplet dimensions.

The hydrogel beads were investigated as carriers for controlled cargo release using encapsulated FITC-dextran. Owing to the supramolecular nature of the hydrogel assembly, fast, triggered


DOI: 10.1021/acs.biomac.5b01048
Biomacromolecules 2015, 16, 2743−2749

release was demonstrated on addition of a competitive guest, with complete release of cargo observed over a matter of minutes. Passive, sustained release of cargo was also demonstrated over 4.5 h. A linear correlation between release rate and CB[8] loading was observed, highlighting the tuneability of the cargo release via the ratio of CB[8] in the hydrogel formulation. Anomalous (non-Fickian) transport is likely to be the predominant release mechanism for these hydrogel beads. The tuneability of the hydrogel bead size, cargo encapsulation, and release kinetics, coupled with their mild and exceedingly simple formation and capacity to be prepared on an industrially relevant scale, highlight these materials as important candidates for use as biocompatible controlled cargo delivery vectors.

## ■ ASSOCIATED CONTENT

### Supporting Information

The bulk preparation of supramolecular hydrogel; images and mean diameter distribution of hydrogel beads fabricated with different flow focus aperture dimensions and different loading of materials; release of different molecular weight FITC-dextran from the formed hydrogel beads; and the determination of enzyme activity in bulk that triggers release from hydrogel beads. The Supporting Information is available free of charge on the ACS Publications website at DOI: 10.1021/acs.biomac.5b01048.

(PDF)
(AVI)
(AVI)
(AVI)

Additional data related to this publication is available at the University of Cambridge data repository (https://www.repository.cam.ac.uk/handle/1810/249249).

## ■ AUTHOR INFORMATION


### Corresponding Authors

*E-mail: ca26@cam.ac.uk.
*E-mail: oas23@cam.ac.uk.


### Notes

The authors declare no competing financial interest.

## ■ ACKNOWLEDGMENTS

This work was supported by the Engineering Physical Sciences Research Council, Translational Grant EP/H046593/1, the Institutional Sponsorship 2012, University of Cambridge EP/K503496/1, a European Research Council Starting Investigator Grant (ASPiRe) ERC-2009-StG-240629, a European Research Council Proof of Concept Grant (SMARTmicroCAPS) ERC-2011-PoC 297504, and an Engineering Physical Sciences Research Council First Grant EP/F035535/1.

## ■ REFERENCES


(1) Appel, E. A.; Biedermann, F.; Rauwald, U.; Jones, S. T.; Zayed, J. M.; Scherman, O. A. *J. Am. Chem. Soc.* **2010**, *132*, 14251−60.
(2) Kisiday, J.; Jin, M.; Kurz, B.; Hung, H.; Semino, C.; Zhang, S.; Grodzinsky, A. J. *Proc. Natl. Acad. Sci. U. S. A.* **2002**, *99*, 9996−10001.
(3) Wan, J. *Polymers* **2012**, *4*, 1084−1108.
(4) Oh, J. K.; Drumright, R.; Siegwart, D. J.; Matyjaszewski, K. *Prog. Polym. Sci.* **2008**, *33*, 448−477.
(5) Peppas, N. A.; Hilt, J. Z.; Khademhosseini, A.; Langer, R. *Adv. Mater.* **2006**, *18*, 1345−1360.
(6) Duncanson, W. J.; Lin, T.; Abate, A. R.; Seiffert, S.; Shah, R. K.; Weitz, D. A. *Lab Chip* **2012**, *12*, 2135−45.
(7) Xu, S.; Nie, Z.; Seo, M.; Lewis, P.; Kumacheva, E.; Stone, H. A.; Garstecki, P.; Weibel, D. B.; Gitlin, I.; Whitesides, G. M. *Angew. Chem., Int. Ed.* **2005**, *44*, 724−8.
(8) Xu, Q.; Hashimoto, M.; Dang, T. T.; Hoare, T.; Kohane, D. S.; Whitesides, G. M.; Langer, R.; Anderson, D. G. *Small* **2009**, *5*, 1575−81.
(9) Rossow, T.; Heyman, J. A.; Ehrlicher, A. J.; Langhoff, A.; Weitz, D. A.; Haag, R.; Seiffert, S. *J. Am. Chem. Soc.* **2012**, *134*, 4983−9.
(10) Sansdrap, P.; Moës, A. J. *Int. J. Pharm.* **1993**, *98*, 157−164.
(11) Zhao, L. B.; Pan, L.; Zhang, K.; Guo, S. S.; Liu, W.; Wang, Y.; Chen, Y.; Zhao, X. Z.; Chan, H. L. *Lab Chip* **2009**, *9*, 2981−6.
(12) Chen, C.-H.; Abate, A. R.; Lee, D.; Terentjev, E. M.; Weitz, D. A. *Adv. Mater.* **2009**, *21*, 3201−3204.
(13) Haghgooie, R.; Toner, M.; Doyle, P. S.12th International Conference on Miniaturized Systems for Chemistry and Life Sciences, San Diego, CA, U.S.A., Oct 12−16, 2008, CBMS: San Diego, CA, 2008.
(14) Seiffert, S.; Weitz, D. A. *Polymer* **2010**, *51*, 5883−5889.
(15) Lewis, C. L.; Lin, Y.; Yang, C.; Manocchi, A. K.; Yuet, K. P.; Doyle, P. S.; Yi, H. *Langmuir* **2010**, *26*, 13436−41.
(16) Hu, Y.; Wang, Q.; Wang, J.; Zhu, J.; Wang, H.; Yang, Y. *Biomicrofluidics* **2012**, *6*, 26502.
(17) Tan, W.-H.; Takeuchi, S. *Adv. Mater.* **2007**, *19*, 2696−2701.
(18) Eun, Y. J.; Utada, A. S.; Copeland, M. F.; Takeuchi, S.; Weibel, D. B. *ACS Chem. Biol.* **2011**, *6*, 260−6.
(19) Kumachev, A.; Greener, J.; Tumarkin, E.; Eiser, E.; Zandstra, P. W.; Kumacheva, E. *Biomaterials* **2011**, *32*, 1477−83.
(20) Sakai, S.; Ito, S.; Inagaki, H.; Hirose, K.; Matsuyama, T.; Taya, M.; Kawakami, K. *Biomicrofluidics* **2011**, *5*, 13402.
(21) Sugaya, S.; Yamada, M.; Seki, M. 16th International Conference on Miniaturized Systems for Chemistry and Life Sciences, Okinawa, Japan, Oct 28 - Nov 1, 2012, CBMS: San Diego, CA, 2012.
(22) Tsuda, Y.; Morimoto, Y.; Takeuchi, S. *Langmuir* **2010**, *26*, 2645−9.
(23) Um, E.; Lee, D.-S.; Pyo, H.-B.; Park, J.-K. *Microfluid. Nanofluid.* **2008**, *5*, 541−549.
(24) Lund, A. W.; Bush, J. A.; Plopper, G. E.; Stegemann, J. P. *J. Biomed. Mater. Res., Part B* **2008**, *87*, 213−21.
(25) Appel, E. A.; del Barrio, J.; Loh, X. J.; Scherman, O. A. *Chem. Soc. Rev.* **2012**, *41*, 6195−214.
(26) Appel, E. A.; Loh, X. J.; Jones, S. T.; Biedermann, F.; Dreiss, C. A.; Scherman, O. A. *J. Am. Chem. Soc.* **2012**, *134*, 11767−73.
(27) Lagona, J.; Mukhopadhyay, P.; Chakrabarti, S.; Isaacs, L. *Angew. Chem., Int. Ed.* **2005**, *44*, 4844−70.
(28) Marquez, C.; Hudgins, R. R.; Nau, W. M. *J. Am. Chem. Soc.* **2004**, *126*, 5806−16.
(29) Liu, S.; Ruspic, C.; Mukhopadhyay, P.; Chakrabarti, S.; Zavalij, P. Y.; Isaacs, L. *J. Am. Chem. Soc.* **2005**, *127*, 15959−67.
(30) Day, A.; Arnold, A. P.; Blanch, R. J.; Snushall, B. *J. Org. Chem.* **2001**, *66*, 8094−100.
(31) Rauwald, U.; Biedermann, F.; Deroo, S.; Robinson, C. V.; Scherman, O. A. *J. Phys. Chem. B* **2010**, *114*, 8606−15.
(32) Kim, J.; Jung, I.; Kim, S.; Lee, E.; Kang, J.; Sakamoto, S.; Yamaguchi, K.; Kim, K. *J. Am. Chem. Soc.* **2000**, *122*, 540−541.
(33) Rauwald, U.; del Barrio, J.; Loh, X. J.; Scherman, O. A. *Chem. Commun.* **2011**, *47*, 6000−2.
(34) Loh, X. J.; del Barrio, J.; Toh, P. P.; Lee, T. C.; Jiao, D.; Rauwald, U.; Appel, E. A.; Scherman, O. A. *Biomacromolecules* **2012**, *13*, 84−91.
(35) Zhang, J.; Coulston, R. J.; Jones, S. T.; Geng, J.; Scherman, O. A.; Abell, C. *Science* **2012**, *335*, 690−694.
(36) Yu, Z.; Zhang, J.; Coulston, R. J.; Parker, R. M.; Biedermann, F.; Liu, X.; Scherman, O. A.; Abell, C. *Chem. Sci.* **2015**, *6*, 4929−4933.
(37) Schneider, C. A.; Rasband, W. S.; Eliceiri, K. W. *Nat. Methods* **2012**, *9*, 671−5.
(38) Ritger, P. L.; Peppas, N. A. *J. Controlled Release* **1987**, *5*, 23−26.
(39) Ritger, P. L.; Peppas, N. A. *J. Controlled Release* **1987**, *5*, 37−42.
(40) Peppas, N. A.; Sahlin, J. J. *Int. J. Pharm.* **1989**, *57*, 169−172.




DOI: 10.1021/acs.biomac.5b01048
*Biomacromolecules* 2015, 16, 2743−2749